






Selection of build orientation for optimal support structures and minimum part errors in additive manufacturing

Paramita Das , Kunal Mhapsekar , Sushmit Chowdhury , Rutuja Samant  and Sam Anand 

Department of Mechanical and Materials Engineering Center for Global Design and Manufacturing University of Cincinnati, Cincinnati, OH 45221

ABSTRACT

Additive Manufacturing (AM) incorporates a group of processes which utilize a layer-based material deposition approach to manufacture parts. These processes are now widely used in the industry as the primary manufacturing process for fabricating high precision parts. The dimensional accuracy of the parts and components manufactured using AM depend mainly on the type of Additive process used and the process parameters. The part build orientation is one of the principal process parameters which has a direct influence on the staircase effect and volume of support structure required for building the part. These factors eventually contribute to the surface finish, dimensional accuracy, and the post-processing requirements. In this paper, an optimization model is developed to obtain the build orientation which will minimize the support structure volume as well as support contact area and maximize the support structure removal while satisfying all the GD&T callouts. The mathematical correlation of cylindricity, flatness, parallelism, and perpendicularity tolerances with build orientation is analyzed and developed. A voxel-based approach is employed to calculate support structure requirement at any part build orientation, while a ray tracing approach is used to calculate the accessibility of supports and identifying removable supports.

KEYWORDS

Additive manufacturing;
build orientation; GD&T;
support structures;
optimization

1. Introduction

Over the last decade, the role of Additive Manufacturing (AM) in the industry has evolved significantly. Starting as an initial rapid prototyping paradigm for inspecting part designs in the early design stages, it has reached a point where AM is being used to fabricate final parts directly from CAD models. AM provides designers with the creative freedom to conceptualize efficient part designs using non-conventional features such as bionic geometries and lattice structures. The capability of AM to manufacture these intricate and complex components in a cost-effective manner provides unprecedented design flexibility to the end user. Variants of the AM process such as Direct Metal Laser Sintering (DMLS), Fused Deposition Modeling (FDM), Electron Beam Melting (EBM) and Selective Laser Sintering (SLS) are being increasingly integrated as the primary fabrication technology in mainstream manufacturing industries. Niche industries such as aviation, medical implants/devices, and electronics are also steadily progressing towards adapting AM as the preferred manufacturing process for products such as aerospace parts, medical implants, and embedded circuits. Many of these parts require precision engineering and adhering to tight GD&T callouts. The performance

monitoring of the manufacturing processes and optimization of their process parameters is thus necessary to satisfy the design requirements and functionality of the component.

AM processes involve the fabrication of a part by the sequential deposition of layers of material. The thickness of the material layer being deposited is known as the slice thickness and it is defined by the user within the limits of the machine. This method of sequential layer deposition introduces a “staircase effect” which gives rise to dimensional errors due to poor surface finish in the final part [8]. AM component designs with overhang features such as pockets, hollow regions, undercuts, holes etc. require support structures to hold up the corresponding layers and those above it during the build process [8] [1] [2] [11]. Support structures also aid in counteracting the thermal deformations occurring in the part during and after the build process. However, support structures are undesirable in the final product as they contribute towards increasing the part weight and post-processing, and thus are removed after the completion of the part build. The machining processes and tools required to remove the support depend on the material used to build the component. The design complexity may

also make it difficult for the tool to reach all the regions of the support structure leading to the incomplete removal of supports during the post processing operations. Furthermore, upon support removal, surfaces of the part in contact with the support structure result in poor surface finish and dimensional inaccuracies. As a result, research on process parameter optimization for AM is identified as critical to ensure the growth of AM towards successful industry integration and mass commercialization. In this regard, the part build orientation, layer thickness and support structure volume are observed to be the important parameters that govern the accuracy and surface quality of the manufactured part [8].

Arni and Gupta [5] evaluated the dependency of flatness error on the part build orientation and developed a mathematical relation between them. Cheng et al. [6] developed a weighted multi-objective optimization function for Stereolithography (SLA) process to optimize the part build orientation. Part accuracy and build time were considered as the critical parameters in this approach. Thompson and Crawford [18] performed a series of experiments to determine the significance of build orientation on the build time, surface finish and part strength for the SLS process. Xu et al. [20] developed an adaptive slicing methodology utilizing genetic algorithm to determine the layer thicknesses at referenced heights of the part. This was combined with an optimization routine to optimize the part build time, part accuracy and stability. Majhi et al. [11] developed a set of geometrical algorithms to minimize the stair step error, support structure volume and support contact area. An empirical model for Stereolithography (SLA) machine accuracy was developed by Lynn-Charney and Rosen [10]. They also developed response surfaces to study the correlation between the part surfaces, tolerances and process variables. Wen et al. [19] investigated the use of particle swarm optimization to perform the simultaneous minimum zone evaluation of cylindricity and conicity errors. Zhang and Li [22] mapped STL facets of a 3D geometry to unit sphere to determine the optimal build direction for each facet. This was followed by a genetic algorithm based search for the global optimal orientation of the part build for the given 3D geometry. Paul and Anand [15] used a graphical approaches to study the correlation between the part build orientation and form errors such as flatness and cylindricity error.

Dutta et al. [8] identified support structure volume minimization as an important parameter for optimizing part quality and minimizing material usage for components manufactured using AM. Allen and Dutta [3] used a ray structures and convex hull based methodology to determine the best build orientation from a candidate set of build orientations for minimizing support

structure volume requirement. Majhi et al. [12] developed computational geometry algorithms to minimize (i) contact-lengths between the part and supports, (ii) area of support structures and the (iii) trapped area for simple polygons. Yang et al. [21] developed a methodology to minimize support structure requirement by considering the difference in area of successive slices during the build of a part in a given orientation. Paul & Anand [15] combined a voxel based approach for support volume calculation with their graphical approaches for determining form errors to conceptualize an optimization model. The result of the optimization model identifies the best build orientation to simultaneously minimize the support volume and part form errors. Das et al. [7] extended Paul & Anand's [15] optimization model by adding graphical relations between other geometric, orientation and runout tolerances along with a Quadtree based algorithm to calculate support structure volume.

The next section presents the methodology involved in determining the individual relationships between build orientation and part form errors, support volume requirement, support contact area and the percentage of support volume removable after the part build has been completed. This is followed by a description of the combined optimization model to optimize the part form errors, support volume, support contact area and percentage of removable supports. The output of this optimization model is the optimum part build orientation which is described in the Results section. The methodology is tested on a test case and the results are discussed. The final section concludes the paper with a brief summary of the work along with the explanation of the impact of this approach, its applications and future scope.

2. Methodology

This section elaborates on the various sub-sections contributing towards the development of the final optimization model. First, the relationship between the part build orientation and GD&T errors for flatness, cylindricity, perpendicularity, and parallelism are established based on previous work [5] [15] [7]. Next the process for calculation of the support structure volume is explained. The voxel-based approach from [15] is adapted to include an angle criteria to generate support structure volumes at different orientations of the part. In the next step, the methodology for identifying and calculating the part surface area in contact with the support structure is elaborated on. This is followed by the use of a ray tracing approach to calculate the percentage of removable supports after the part has been built. Finally, all these components are integrated into a weighted combined objective function for the proposed optimization

routine. The orientation of the part about the x and y-axes (α and β) serve as the optimization variables in the combined optimization model.

2.1. Relationship between GD&T errors and build orientation

The GD&T tolerances considered for the proposed optimization routine are (i) Flatness, (ii) Cylindricity, (iii) Perpendicularity and (iv) Parallelism. We begin by introducing the individual form tolerance errors and their correlation with the build orientation. The standard definitions of the aforementioned tolerances as outlined by ASME are as listed below [4]:

Flatness tolerance/error (ε_f) of a surface is mathematically defined as the minimum separation between a pair of parallel planes which encompass all the points on the given surface, between them.

Cylindricity tolerance/error (ε_{cyl}) is defined as the zone between two co-axial cylinders within which all the points of the given surface must lie.

Perpendicularity tolerance/error (ε_{per}) is defined as the minimum tolerance zone defined two parallel planes perpendicular to a datum plane, within which all the points sampled from a given surface are enclosed.

Parallelism tolerance/error (ε_{para}) is defined as the minimum tolerance zone defined by two parallel planes which are parallel to a datum plane and contain all the

sampled points from a surface with the parallelism tolerance requirement.

Fig. 1, shows the examples of different tolerance call outs on sample parts.

Previous works in this domain have established the relationship between the part build orientation and the resulting tolerance errors for a given slice thickness Δz . These are discussed below.

The relation between the build orientation of a surface and the resulting flatness error ε_f as established by Arni and Gupta [5] is given as:

$$\varepsilon_f = \Delta z \cos(\theta_f) \quad (1)$$

Where θ_f is the angle between the build axis (z-axis) and the normal of the surface with flatness tolerance.

Paul and Anand [15] established the relationship between the build orientation and the resulting cylindricity error (ε_{cyl}) as:

$$\varepsilon_{cyl} = \Delta z \sin(\theta_{cyl}) \quad (2)$$

Where, θ_{cyl} is the angle made by the axis of the cylindrical feature with the build axis (z-axis).

Das et al. [7] established the relationship between perpendicularity and parallelism errors and the build orientation as:

$$\varepsilon_{per} = \Delta z \cos(\theta_{per}) \quad (3)$$

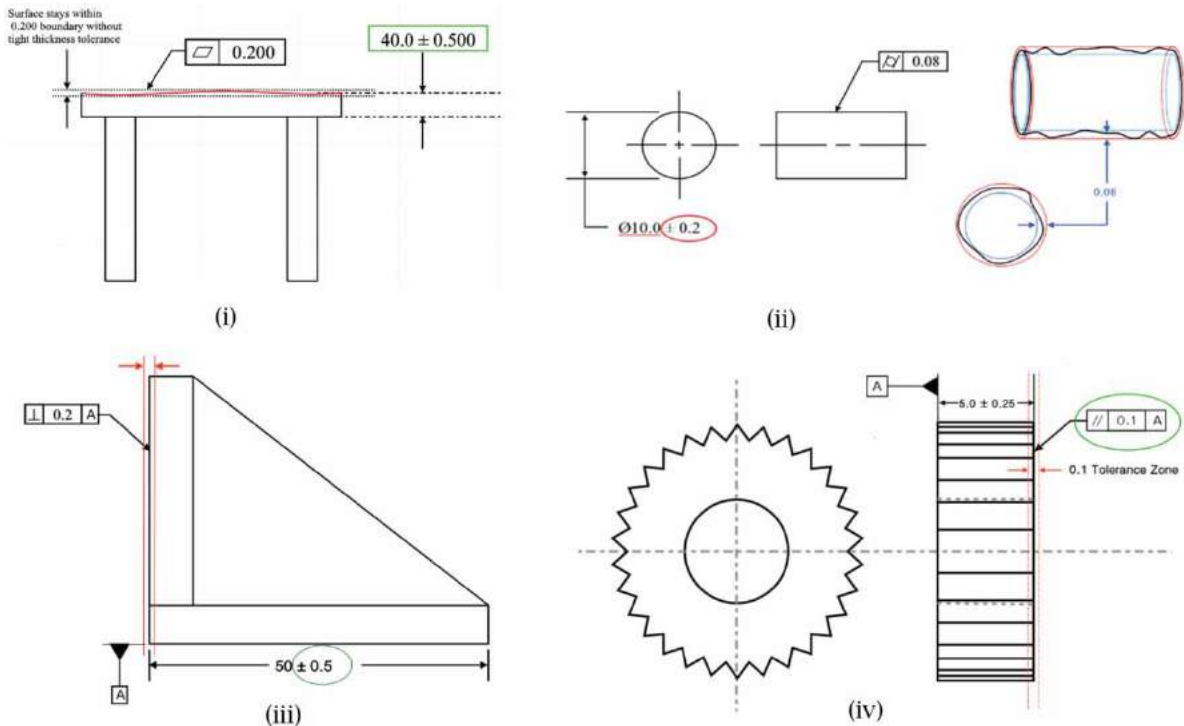


Figure 1. Examples of tolerance call outs on given surfaces. (i) Flatness, (ii) Cylindricity, (iii) Perpendicularity and (iv) Parallelism. (Images adapted from [9]).

$$\varepsilon_{para} = \Delta z \cos(\theta_{para}) \quad (4)$$

Where, θ_{per} is the angle between the build axis (z-axis) and the normal of the surface with the perpendicularity constraint and θ_{para} is the angle made by the normal of the given surface with the build axis direction (z - axis).

2.2. One dimensional tolerance maps

Paul & Anand [15] used the above relationships between the build orientation and tolerance errors to develop one-dimensional tolerance maps for flatness and cylindricity tolerances. These maps are defined in terms of cosines of θ_f and θ_{cyl} . When represented on a number line, they divide the interval between 0 and 1 into feasible and infeasible regions for the respective tolerances. Das et al. [7] further extended this approach for perpendicularity, parallelism, angularity and conicity tolerances. In this section, a brief explanation of Paul and Anand's [15] methodology to generate the one-dimensional tolerance map for flatness tolerance is presented here.

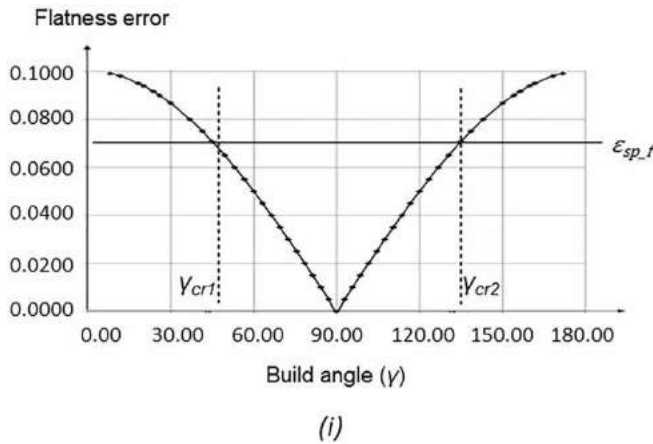
Consider a part having n_f critical planar features. Let the i^{th} planar feature have a flatness tolerance call out of $\varepsilon_{sp_f}^i$. Fig. 2 (i) shows the plot of flatness error $\varepsilon_{sp_f}^i$ in the i^{th} planar feature of the part vs the part build orientation with respect to the build direction (z-axis). As shown in the figure, the flatness error of the given planar feature will satisfy the defined flatness tolerance if the angle (ψ_f^i) between the surface normal (\vec{n}_f^i) and the build direction (\vec{v}) lies within the critical regions. This is represented mathematically as [15]:

$$(\psi_{cr1})_f^i \leq \psi_f^i \leq (\psi_{cr2})_f^i \quad (5)$$

$$\Rightarrow (\psi_{cr1})_f^i \leq \psi_f^i \leq 180 - (\psi_{cr1})_f^i \quad (6)$$

Taking cosines on both sides for equation [6] we get:

$$-\cos((\psi_{cr1})_f^i) \leq \cos(\psi_f^i) \leq \cos((\psi_{cr1})_f^i) \quad (7)$$



$$\Rightarrow -(a_{cr})_f^i \leq (a_z)_f^i \leq (a_{cr})_f^i \quad (8)$$

Squaring both sides,

$$0 \leq (a_z^2)_f^i \leq (a_{cr}^2)_f^i \quad (9)$$

Thus, the feasible build orientations to build the part while satisfying the flatness tolerance callout of the planar feature can be represented on a 1D line as shown in Fig. 2 (ii).

Considering a part with multiple planar features, the optimal build orientation of the part will be one in which the z-component of each surface normal of all planar features lie within the defined feasible region on the 1D map. If the planar features do not satisfy the individual feasible orientation requirements, a penalty is imposed on the individual features. The penalty for flat features is as shown in Fig. 2 (iii) and is mathematically defined as:

$$p_{flat} = (a_z^2)_f^i \quad (10)$$

Similarly, Paul & Anand [15] developed the penalty function for cylindricity as:

$$p_{cyl} = 1 - (a_z^2)_{cyl}^i \quad (11)$$

Das et al. [7] extended the above approach to determine the penalty function for perpendicularity and parallelism tolerances as:

$$p_{per} = (a_z^2)_{per}^i \quad (12)$$

$$p_{para} = (a_z^2)_{para}^i \quad (13)$$

2.3. Volume of support structure

Support structures are required in the layer-by-layer build process to support the overhang features and the material deposited above the overhangs. In some designs, support structures also reduce the thermal deformations

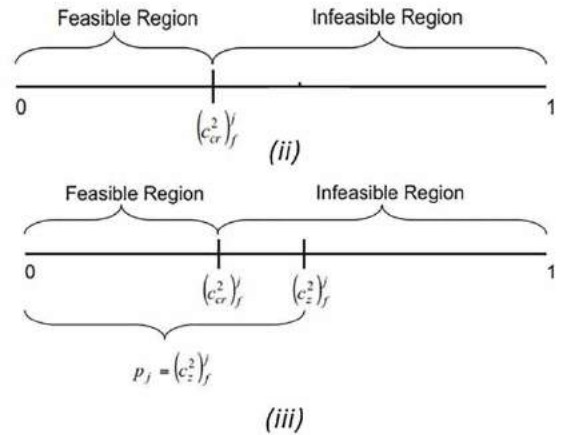


Figure 2. (i) Plot of Flatness error vs build angle, (ii) One dimensional map for flatness error, (iii) Penalty for flat features (Adapted from [5] and [15]).

in the part. Overall, support structures are required to build a stable part in a given orientation. Paul and Anand [15] used a voxel-based approach to generate support from part STL file. The STL file is a standard file format used by AM machines and consists of planar triangular tessellated representation of the part. The approach from [15] has been adapted in this work to create support structure with the addition of an angle criterion. The angle criterion is a user-defined threshold set on the orientation of the features of the part with respect to the build orientation. Depending on the additive process and the material used, not all the overhung features require support. If the negative slope of the feature's surface is steeper than the defined critical angle, then the feature is deemed capable of supporting the successive layers of material on top of it and hence supports are not required. In this work, the threshold for the angle criterion is set to 45° . This implies that the surfaces oriented at an angle greater than 45° with the build direction need support. This can also be checked in terms of the surface normal, i.e. if the surface normal of a given facet makes an angle greater than 135° with positive Z-axis, it requires support.

The implementation of the threshold angle criterion on the part's STL file is explained here. The facet normals making an angle of 135° with the Z-axis (build direction) are first identified. The corresponding facets are then finely discretized into points at equal intervals. A bounding box for the part is determined using the STL coordinates of the STL vertices and the entire space of the bounding box is populated with empty voxels of user-defined size. Then, for each of the discretized point on the support requiring facet, an empty voxel is identified which contains that point and is marked as a support voxel. All such support voxels are identified. Simultaneously, the STL part file is being converted into its voxel approximation [17] [14]. In the next step, the algorithm traverses from each of the support voxels towards the defined substrate level (usually $Z = 0$), and each empty voxels that it encounters during the traversal is also identified as a support voxel. If however a part voxel is encountered in the path, the traversal is terminated. In this way, all the support structure voxels for the given part are identified accurately. The test cases demonstrated in Fig. 3 and Fig. 4 represent the voxelized support

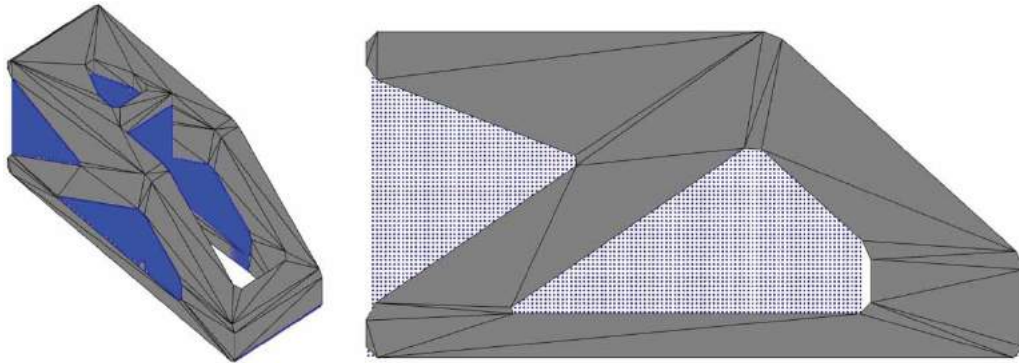


Figure 3. Voxel representation of support structure for cantilever beam.

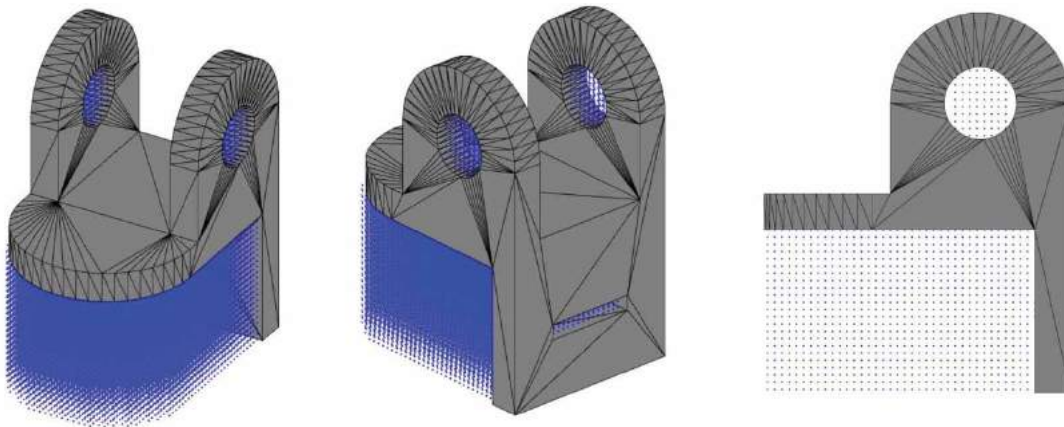


Figure 4. Voxel representation of support structures for bracket.

structure for respective parts. Each blue point represents the centroid of the support voxel.

2.4. Calculation of support contact area

The surface area of the part in contact with the support structure is seen to have poor surface finish after the support has been removed. The support contact area directly depends on the features and surfaces of the part which require support as well as the part build direction. Whether a feature requires support or not is dependent on its orientation with respect to the build direction.

In our approach, the STL file of the part is analyzed for support requirement. Along with the facet vertices, the STL file also comprises of the information about normal vectors of all the triangular facets. Ranjan et al. [16] developed an algorithm to calculate the contact area of the supports. The angle made by each facet normal with respect to the build axis (Z-axis) is evaluated and the facets whose normal vectors make an angle of more than 135° are identified as the facets which require support. However, these are not the only facets that are in contact with the support structure. The part facets which are right underneath the supports, as well as the vertical facets which are adjacent to support structure, should also be considered as support contact facets. Fig. 5 shows the three types of support contact facets along with the voxelized representation of the support structure in contact with these surfaces.

The area of all the STL facets requiring support is calculated using the vector cross product of the facet edges. To determine the support contact area resulting from facets which are right underneath the support requiring facets, each of the support requiring facets is evaluated

separately. If an upward facing facet is identified to be right underneath a support requiring facet, then the area of the support requiring facet is projected on the plane of the upward facing facet. The overlap between the areas of these two facets is stored as the required intersection area in contact with support structure. Furthermore, the facets that are adjacent to the support facets and are vertical, also touch the support structure. To take this into account, the facets that share an edge with any of the support contact facets and have facet normal perpendicular to the build direction, i.e. in the XY plane, are also identified as support contact facets and their area is determined. Finally, the areas of all the support requiring facets, upward facing contact facets and vertical contact facets are summed up to get the total support contact area. Fig. 6 explains the algorithm in detail.

2.5. Support structure removal

For features such as overhangs, horizontal undercuts and drafts, the support structures are inevitable during the build process. However, once the part is built, there is no more utility for the supports and hence, support structures must be removed during the post-processing operations. Various methods are used to remove the support structure depending on the material. Electric Discharge Machining (EDM) is widely used to remove metallic supports. For polymers, chemical etching and dissolution are used. Depending on the support removal process, tool geometry and complexity of the part geometry, the percentage of removable support structure may vary. Since the extent of accessibility of supports for eventual removal depends on the build orientation, determining optimal build orientations for maximizing support removal is crucial.

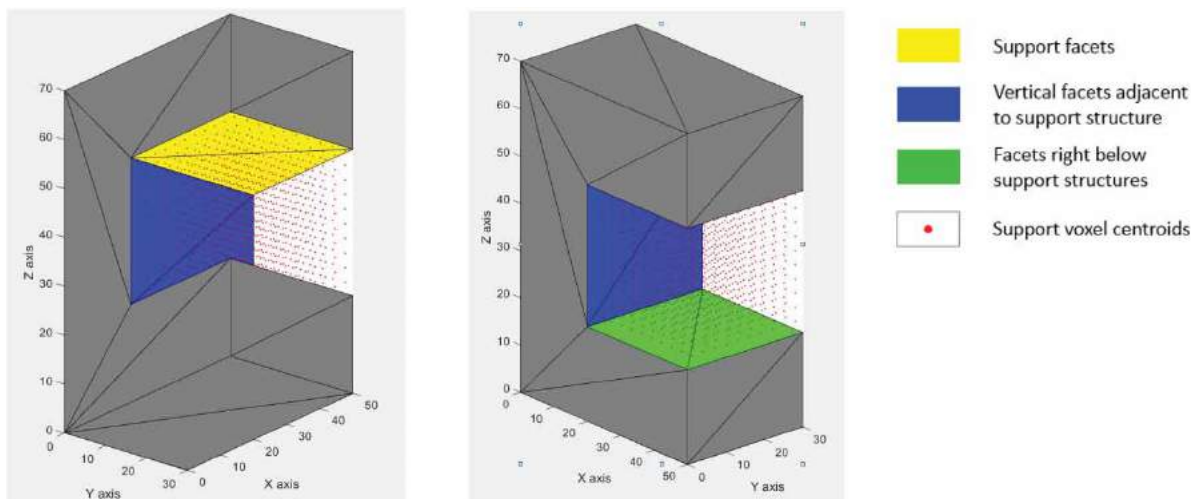


Figure 5. Representation of support contact area using facets.

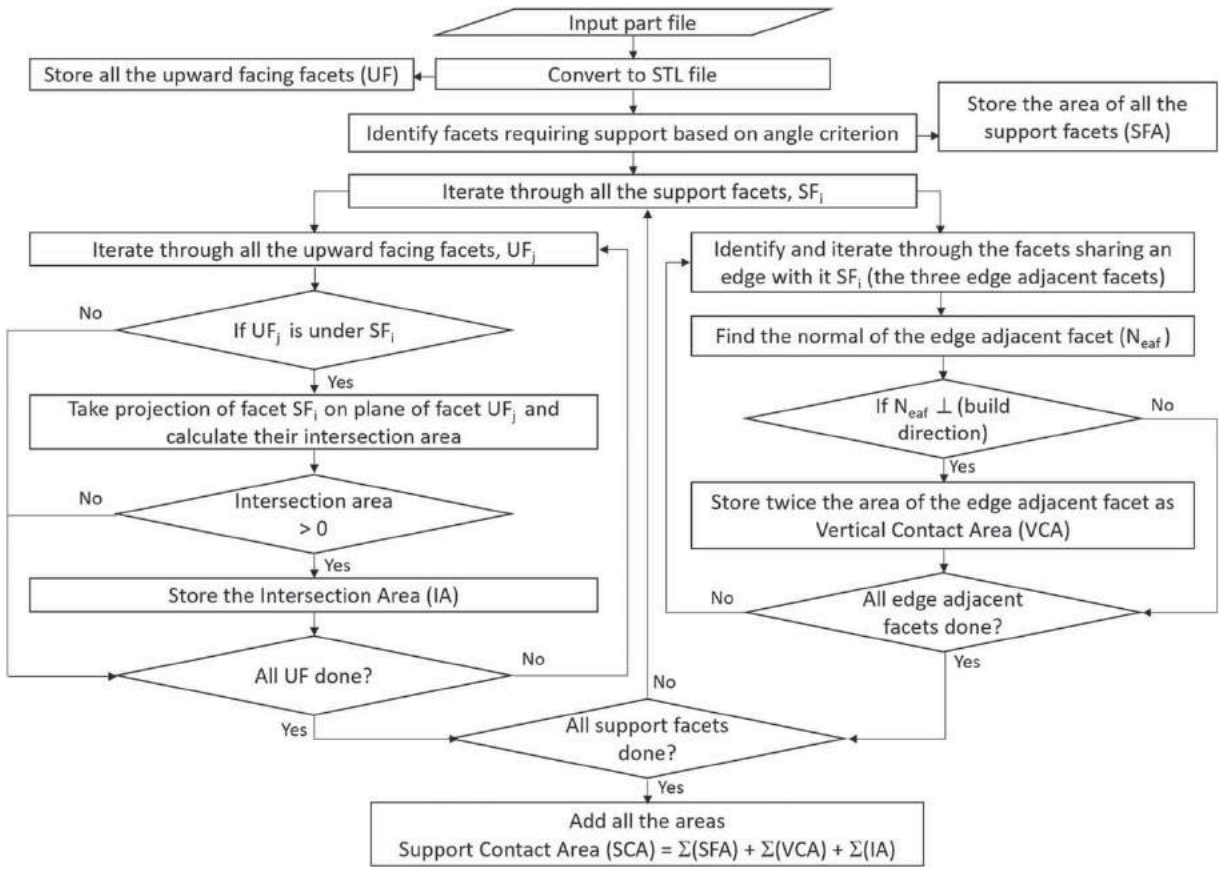


Figure 6. Algorithm for calculation of support contact area.

In this work, six directions along the coordinate axes are considered for removal of support structures (Fig. 7) to simulate the tool's accessibility. It is assumed that a linear tool is used along these directions to cut off the support. The voxelized support generated in section 2.1 is considered here. Data regarding voxel positions in the voxelized space and the size of the voxels are used to calculate the centroid of each voxel. The algorithm iterates through each voxel centroid and considers it as the ray origin. From this ray origin, rays are traced in six directions along the negative Z-axis, Z-axis, X-axis, negative X-axis, Y-axis, and negative Y-axis, respectively. Fig. 8 represents the voxel centroids and the six directional rays for an overhang feature requiring support.

Each of these rays is checked for intersection with each of the part STL facets. If a ray intersects any of the part facets, then that voxel is deemed not accessible or removable from the direction of the intersecting ray, i.e. the part is hindering the path of the tool along that ray towards that voxel. In this manner, access to the support voxel along each ray direction is checked. If a ray does not intersect any of the part facets, it is accessible for removal in that direction. The same procedure is repeated for all support voxels. If for a voxel, all the six rays intersect with the part STL facet, then that support voxel is

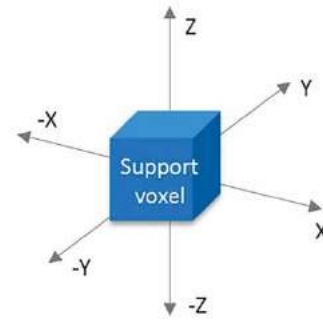


Figure 7. Six directions for support structure removal check.

deemed inaccessible. These inaccessible voxels contribute towards non-removable support volume (V_{NRS}) which is calculated as the product of number of inaccessible voxels (N_{iv}) times the volume of each voxel (V_v) and is given by:

$$V_{NRS} = N_{iv} \times V_v \quad (14)$$

The score for removable support (RS), i.e. the percentage of the removable support is calculated as follows:

$$RS = (V_S - V_{NRS}) / V_S \times 100 \quad (15)$$

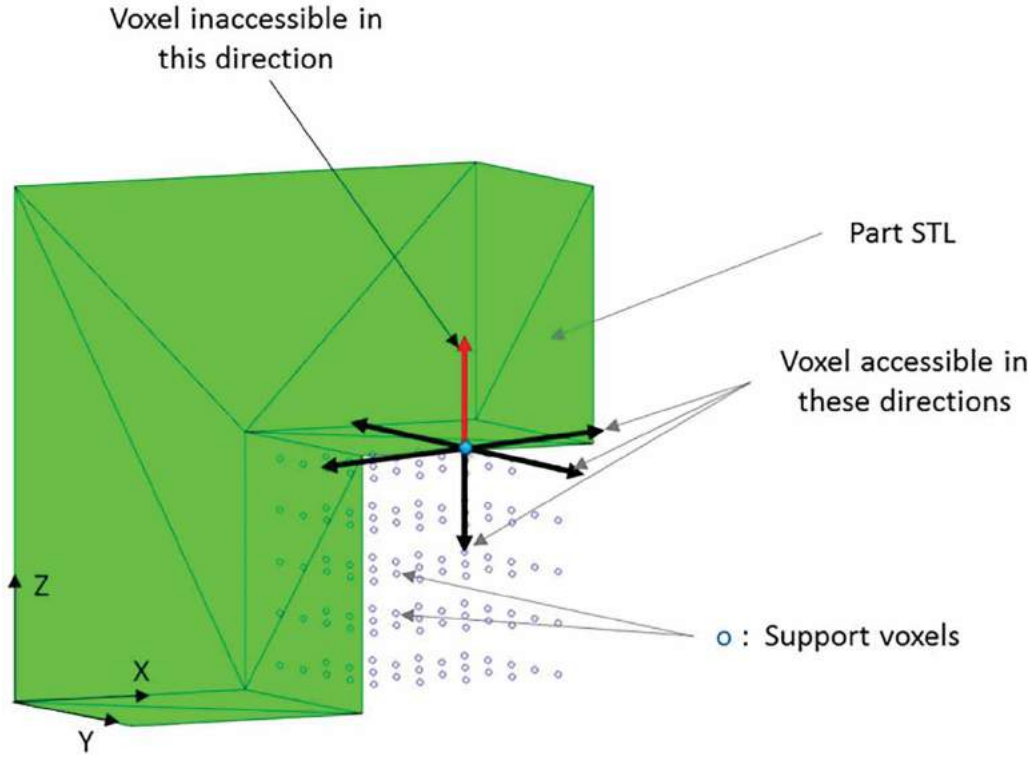


Figure 8. Ray tracing approach to analyze removal of support structure.

This score for support structure removal is later used in the combined optimization model to identify the best build orientation. Fig. 9 shows the test cases in the support removal analysis along with their respective removal scores. Different part geometries are considered in the case studies to demonstrate the robustness of the algorithm.

2.6. Optimization model

Previous sections (2.1 to 2.4) explained the methodology for calculating the values and parameter scores for GD&T errors and support structure parameters at a fixed build orientation. All these parameters are completely independent of each other and have different values at different build orientations. Real life applications call for optimization of support structures while minimizing geometric errors as a function of build orientation. However, optimum supports and minimum GD&T errors may be found at different build orientations. Therefore, a combined optimization model is necessary to obtain the best part build orientation at which all the parameters are simultaneously optimized.

A combined multi-objective optimization model is developed with the build orientation as the variable [15] [7]. Build orientation is represented in terms of (α, β) , where α is the angle by which the part is rotated about

X axis and β is the angle of rotation about the Y axis. The objective function is a combined error function with a minimization objective, as given in equation (19). Within the objective function, the values of individual parameters are represented in the form of normalized penalty functions. The penalty functions for geometric errors have been previously developed in section 2.1. Support contact area is normalized by dividing it by the total part surface area and its penalty function (p_{SCA}) is shown in equation (16). The normalized penalty for support structure volume (p_{SV}) is calculated using equation (17) given by Paul and Anand [15] where, V_{s_min} and V_{s_max} are the minimum and maximum values of support volume calculated, using the approach explained in section 2.2. The technique discussed in section 2.4 gives the support removal score (SR) as a percentage value. Therefore, to integrate this score into the objective function, the penalty for non-removable support (p_{SR}) is calculated using equation (18).

$$p_{SCA} = \text{Support contact area} / \text{Total surface area} \quad (16)$$

$$p_{SV} = V_{s_norm}(\alpha, \beta) = \frac{V_s(\alpha, \beta) - V_{s_min}}{V_{s_max} - V_{s_min}} \quad (17)$$

$$p_{SR} = (100 - SR) / 100 \quad (18)$$

The normalized penalties are weighted and aggregated in the final minimization objective function $E(\alpha, \beta)$ [7].

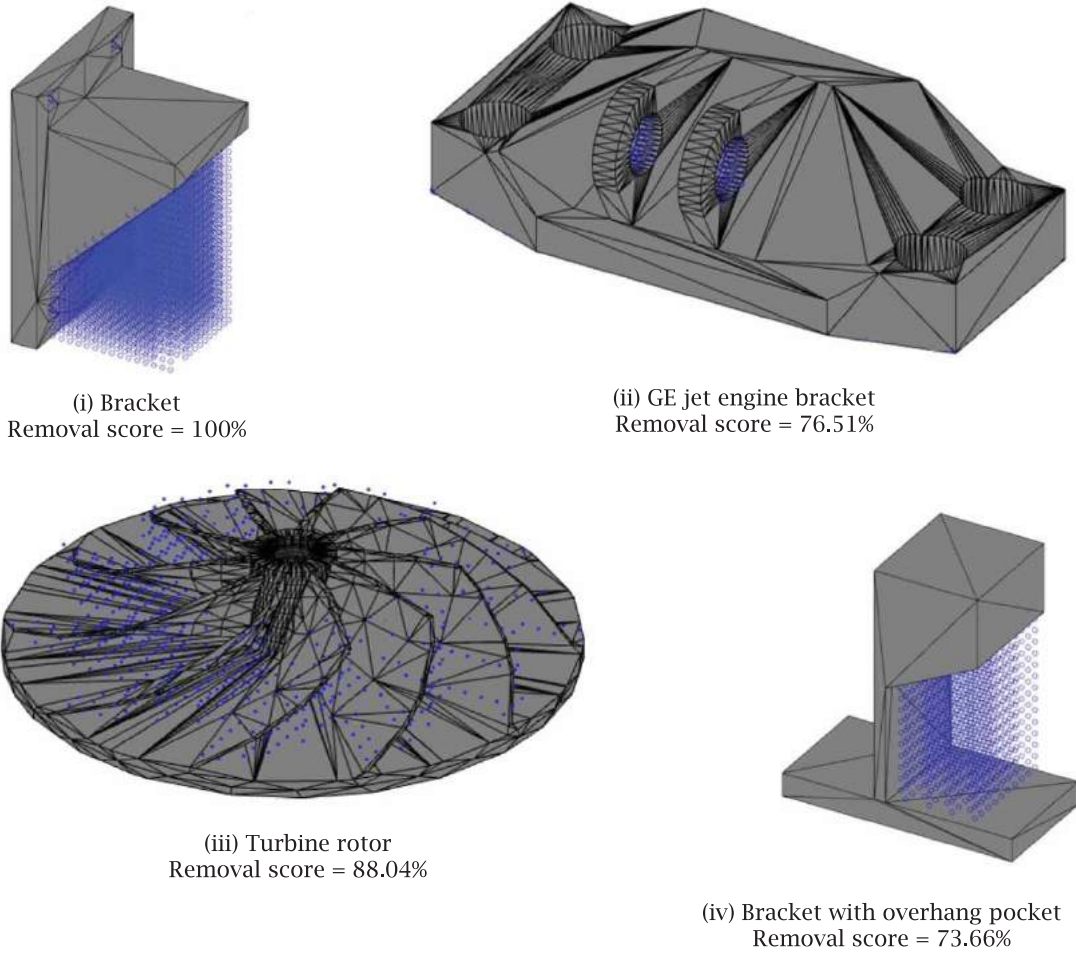


Figure 9. Test cases for support structure removal

The weights provide the flexibility to vary the effect of the individual penalties of the design parameters on the objective function. Equations (20) to (23) show the optimization constraints related to the GD&T errors. The lower and upper bounds on α and β are given in equations (24) and (25). The complete optimization problem is shown below.

Minimize,

$$E(\alpha, \beta) = \sum_{i=1}^{ncyl} w_i p_i + \sum_{j=1}^{nf} w_j p_j + \sum_{k=1}^{nper} w_k p_k + \sum_{l=1}^{npara} w_l p_l + w_{SCA} p_{SCA} + w_{SV} p_{SV} + w_{SR} p_{SR} \quad (19)$$

Such that,

$$(a_{cr}^2)_{cyl}^i \leq (a_z^2)_{cyl}^i \leq 1, \text{ where } i = 1, 2 \dots n_{cyl} \quad (20)$$

$$0 \leq (a_z^2)_f^j \leq (a_{cr}^2)_f^j, \text{ where } j = 1, 2 \dots n_f \quad (21)$$

$$0 \leq (a_z^2)_{per}^k \leq (a_{cr}^2)_{per}^k, \text{ where } k = 1, 2 \dots n_{per} \quad (22)$$

$$0 \leq (a_z^2)_{para}^l \leq (a_{cr}^2)_{para}^l, \text{ where } l = 1, 2 \dots n_{para} \quad (23)$$

$$0^\circ \leq \alpha \leq 360^\circ \quad (24)$$

$$0^\circ \leq \beta \leq 360^\circ \quad (25)$$

$$\sum_{i=1}^{ncyl} w_i + \sum_{j=1}^{nf} w_j + \sum_{k=1}^{nper} w_k + \sum_{l=1}^{npara} w_l + w_{SCA} + w_{SV} + w_{SR} = 1 \quad (26)$$

The defined optimization problem is solved using the `fmincon` routine from MATLAB (2015), which is a gradient-based method that uses sequential quadratic programming [13]. The output of the optimization model is the optimum build orientation for the given part in terms of α_{opt} and β_{opt} . α_{opt} is the angle by which the part is to be rotated about X axis and β_{opt} is the angle by which the part is to be rotated about Y-axis to get the final part build orientation.

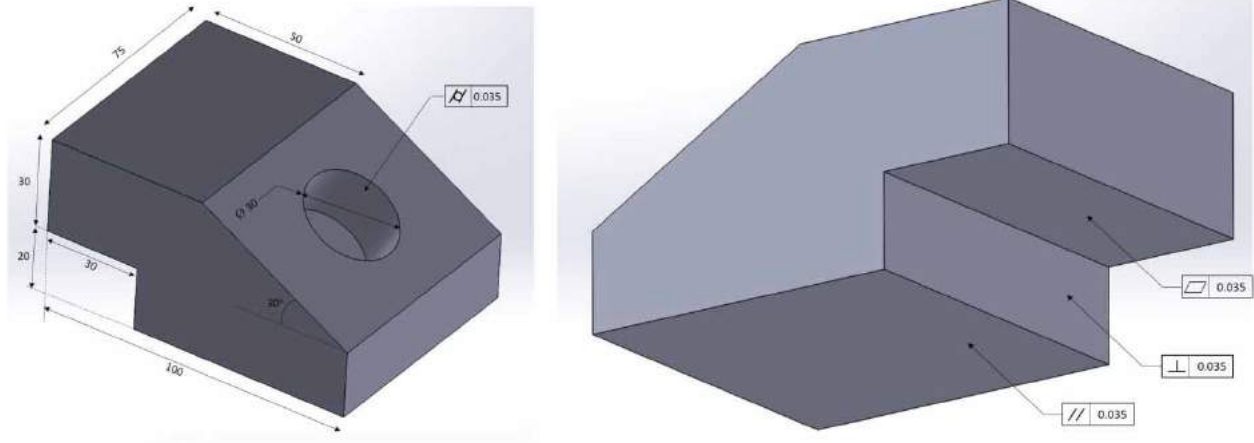


Figure 10. Test part: dimensions and tolerance callouts.

3. Results

The optimization model developed in the previous section is used to determine the best build orientation for a test part shown in Fig. 10. The test part has 1 feature each with cylindricity, flatness, parallelism and perpendicularity callouts. The tolerance values for each of the four GD&T callouts is manually set as 0.035 millimeters. The dimensions of the part and the part features corresponding to each tolerance callout are shown in Fig. 10. The minimum and maximum volume of support structure for the test part are 0 mm^3 and 247455 mm^3 respectively. These were calculated by rotating the part sequentially in steps of 15° through all possible orientations and using the voxel-based approach for support volume calculation. These values are used to normalize the support volume penalty function for this part. Total surface area of the part is calculated by summing the STL facet areas and is determined to be 30154 mm^2 . This value is used to normalize the penalty function for support contact area.

A fixed slice thickness of 0.05 mm ($50 \text{ }\mu\text{m}$) is used in all the runs of the optimization model. Angles of rotation about X and Y axes are varied from 0° to 360° . Three test runs of the optimization routine are carried out for the

given part to study the effect of changing the parameter weights on the resulting optimal orientation of the part. The results are presented in the following sections.

3.1. Test run 1

For test run 1, we used a weight value of 0.1 for support contact area and equal weights of 0.15 for rest of the parameters. For the preset values of slice thickness and weights, the optimum build orientation is obtained as $\alpha_{\text{opt}} = 111.56^\circ$ and $\beta_{\text{opt}} = 43.97^\circ$ with the minimum value of the objective function as $E_{\text{min}} = 0.0144$. Values of each parameter at the optimum build orientation are calculated and tabulated in Table 1. Voxel representation of support structure required in the optimum build orientation is shown in Fig. 11 (i). Fig. 11 (ii) shows the bottom view of the STL representation of the part in the optimum build orientation and the facets of the STL that require support. The positive Z axis is taken as the build direction. It is clear from the results in Table 1 that all the tolerance callouts are satisfied except cylindricity. Consequently, in the next test run weights are modified and the weight of the penalty function for cylindricity callout is increased.

Table 1. Test part first run: optimum build orientation and parameter values

Parameter	Weights		Tolerance callouts	Final parameter values: test run 1	Optimal orientation	
					α_{opt}	β_{opt}
Cylindricity	w_{cyl}	0.15	0.035 mm	0.041 mm	111.56°	43.97°
Flatness	w_f	0.15	0.035 mm	0.013 mm		
Perpendicularity	w_{per}	0.15	0.035 mm	0.035 mm		
Parallelism	w_{para}	0.15	0.035 mm	0.013 mm		
Support contact area	w_{SCA}	0.1	–	348.32 mm^2		
Support structure volume	w_{SV}	0.15	–	15080 mm^3		
Support removal percentage	w_{SR}	0.15	–	98.46 %		

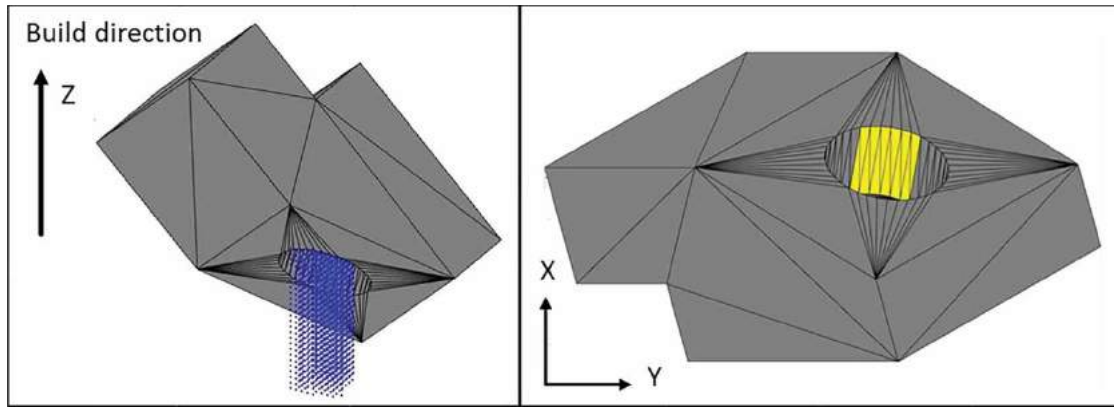


Figure 11. Test part in optimum build orientation: test run 1.

Table 2. Test part first run: optimum build orientation and parameter values.

Parameter	Weights		Tolerance callouts	Final parameter values: test run 1	Final parameter values: test run 2	Optimal orientation	
						α_{opt}	β_{opt}
Cylindricity	w_{cyl}	0.5	0.035 mm	0.041 mm	0.031 mm	226.68°	36.70°
Flatness	w_f	0.1	0.035 mm	0.013 mm	0.027 mm		
Perpendicularity	w_{per}	0.05	0.035 mm	0.035 mm	0.029 mm		
Parallelism	w_{para}	0.1	0.035 mm	0.013 mm	0.027 mm		
Support contact area	w_{SCA}	0.1	–	348.32 mm ²	6798 mm ²		
Support structure volume	w_{SV}	0.1	–	15080 mm ³	112050 mm ³		
Support removal percentage	w_{SR}	0.05	–	98.46%	97.18%		

3.2. Test run 2

The second set of results is obtained by providing a greater weight to the cylindricity callout. The weight for penalty function of cylindricity (w_{cyl}) is set to be 0.5 and the flatness, parallelism and perpendicularity callouts are weighted by 0.1, 0.1 and 0.05, respectively. Weights for support structure volume and support contact area are given a value of 0.1 and the penalty function for support removal is weighted by 0.05. Slice thickness is kept fixed at 0.05 mm. The upper and lower bounds on the values of α and β are also kept fixed as 0° and ° and 360°, respectively. The results of test run 2, including the optimum part build orientation and values of the parameters at that build orientation, are tabulated in Table 2.

The optimum orientation with the new set of weights is obtained as $\alpha_{opt} = 226.68^\circ$ and $\beta_{opt} = 36.70^\circ$ with the minimum value of the objective function as

$E_{min} = 0.0611$. It is observed that the cylindricity error at this build orientation is reduced by 24% and is within tolerance limits. The rest of the tolerance callouts are also satisfied. Due to the increased weight of cylindricity tolerance, it is inferred that a higher priority is given to minimize the cylindricity error. It is also observed that because the weights of the support structure parameters are lower than those in the first test run, the values of these parameters are higher in the optimal orientation from Test Run 2 as compared to the Test Run 1.

3.3. Test run 3

In the third test run, the support structure parameters are given a higher weight and the weights for GD&T parameters are reduced. This test run demonstrates how the weights change the influence of individual parameters on the combined optimization function and the solution.

Table 3. Test part third run: optimum build orientation and parameter values.

Parameter	Weights		Tolerance callouts	Final parameter values: test run 1	Final parameter values: test run 2	Optimal orientation	
						α_{opt}	β_{opt}
Cylindricity	w_{cyl}	0.05	0.035 mm	0.041 mm	0.036 mm	134.81°	189.71°
Flatness	w_f	0.05	0.035 mm	0.013 mm	0.034 mm		
Perpendicularity	w_{per}	0.05	0.035 mm	0.035 mm	0.008 mm		
Parallelism	w_{para}	0.05	0.035 mm	0.013 mm	0.034 mm		
Support contact area	w_{SCA}	0.3	–	348.32 mm ²	268 mm ²		
Support structure volume	w_{SV}	0.35	–	15080 mm ³	2970 mm ³		
Support removal percentage	w_{SR}	0.15	–	98.46 %	64.54 %		

Table 3 shows values of the weights and the optimum orientation obtained using those weights. The values of all the parameters at the new optimum build orientation are also listed in the table.

With a higher weightage to the support structure parameters, the optimum build orientation is obtained as $\alpha_{\text{opt}} = 134.81^\circ$ and $\beta_{\text{opt}} = 189.71^\circ$. At this optimum part build orientation, the support structure volume is 2970 mm^3 which is 80.3% less than that in the first test run results. Support contact area is also reduced by 23%. The weights of GD&T parameters are comparatively lower which result in an increase in the flatness and parallelism errors. Moreover, only three of the four GD&T callouts are satisfied due to low respective weights. It is inferred that the relatively higher weights of support parameters prioritized minimization of those parameters over the GD&T callouts. Therefore, the support structure requirement is primarily reduced in order to minimize the objective function.

4. Conclusion

A comprehensive additive manufacturing part quality optimization routine has been presented in this paper. The routine returns the best build orientation for the given component to satisfy the user-defined thresholds for flatness, cylindricity, perpendicularity and parallelism tolerances for the different features in the given part. Simultaneously, the support volume requirement is optimized such that the volume of support required and support contact area are minimized while the percentage of removable support structure material is maximized. Three test runs of the routine were implemented on an example part with varied weights for each individual parameter. The results of the test runs validate that the optimum build orientation is dependent on the priority given to the individual design parameters in the form of weights.

In the future, the proposed optimization routine can be extended to include other quality parameters such as conicity, angularity, runout tolerances etc. More comprehensive solutions can also be obtained by including various AM design considerations and part properties which are dependent on build orientation.

ORCID

Paramita Das  <http://orcid.org/0000-0002-3823-0149>

Kunal Mhapsekar  <http://orcid.org/0000-0002-8795-8734>

Sushmit Chowdhury  <http://orcid.org/0000-0002-8092-7003>

Rutuja Samant  <http://orcid.org/0000-0001-9622-9720>

Sam Anand  <http://orcid.org/0000-0001-5925-8258>

References

- [1] Allen, S.; Dutta, D.: Determination and evaluation of support structures in layered manufacturing, *Journal of Design and Manufacturing*, 5(3), 1995, 153–162. [http://dx.doi.org/10.1016/S0010-4485\(97\)00083-3](http://dx.doi.org/10.1016/S0010-4485(97)00083-3)
- [2] Allen, S.; Dutta, D.: Wall thickness control in layered manufacturing for surfaces with closed slices, *Computational Geometry*, 10(4), 1998, 223–238. [http://dx.doi.org/10.1016/S0925-7721\(98\)00009-1](http://dx.doi.org/10.1016/S0925-7721(98)00009-1)
- [3] Allen, S.; Dutta, D.: On the computation of part orientation using support structure in layered manufacturing, *Solid Freeform Fabrication Symposium*, Austin, 1994.
- [4] ASME, American National Standards Institute, Dimensioning and Tolerancing for Engineering Drawings, ANSI Standard Y14.5M, 1994.
- [5] Arni, R.; Gupta, S.: Manufacturability analysis of flatness tolerances in solid freeform fabrication, *Journal Of Mechanical Design*, 123(1), 2001, 148–156. <http://dx.doi.org/10.1115/1.1326439>
- [6] Cheng, W.; Fuh, J.; Nee, A.; Wong, Y.; Loh, H.; Miyazawa, T.: Multi objective optimization of part building orientation in stereolithography, *Rapid Prototyping*, 1(4), 1995, 12–23. <http://dx.doi.org/10.1108/13552549510104429>
- [7] Das, P.; Chandran, R.; Samant, R.; Anand, S.: Optimum Part Build Orientation in AM for Minimizing Part Errors and Support Structures, *Proceedings of NAMRI/SME*, Charlotte, NC, 1, 2015, 343–354. [doi:10.1016/j.promfg.2015.09.041](https://doi.org/10.1016/j.promfg.2015.09.041)
- [8] Dutta, D.; Kulkarni, P.: A review of process planning techniques in layered manufacturing, *Rapid Prototyping Journal*, 6(1), 2000, 16–35. <http://dx.doi.org/10.1108/13552540010309859>
- [9] GD&T basics, <http://www.gdandtbasics.com/gdt-symbols/>.
- [10] Lynn-Charney, C.; Rosen, D.W.: Usage of accuracy models in stereolithography process planning, *Rapid Prototyping Journal*, 6(2), 2000, 77–86. <http://dx.doi.org/10.1108/13552540010323600>
- [11] Majhi, J.; Janardan, R.; Smid, M.; Gupta, P.: On some Geometric Optimization Problems in Layered Manufacturing, *Computational Geometry*, 12(3–4), 1998, 219–239. [http://dx.doi.org/10.1016/S0925-7721\(99\)00002-4](http://dx.doi.org/10.1016/S0925-7721(99)00002-4)
- [12] Majhi, J.; Janardan, R.; Schwerdt, J.; Smid, M.; Gupta, P.: Minimizing support structures and trapped area in two-dimensional layered manufacturing, *Computational Geometry*, 12(3–4), 1999, 241–267. [http://dx.doi.org/10.1016/S0925-7721\(99\)00003-6](http://dx.doi.org/10.1016/S0925-7721(99)00003-6)
- [13] MathWorks Matlab Support, <http://www.mathworks.com/help/optim/ug/fmincon.html>.
- [14] MATLAB, Mathworks, http://www.mathworks.com/Mesh_Voxelization_Code
- [15] Paul, R.; Anand, S.: Optimization of Layered manufacturing process for reducing form errors with minimal support structures, *Journal of Manufacturing Systems*, 36, 2014, 231–243. <http://dx.doi.org/10.1016/j.jmsy.2014.06.014>
- [16] Ranjan, R.; Samant, R.; Anand, S.: Design for Manufacturability in Additive Manufacturing Using a Graph Based Approach, *ASME 2015 International Manufacturing*

- Science and Engineering Conference, Charlotte, North Carolina, USA, 2015.
- [17] Subburaj, K.; Patil, S. S.; Ravi, B.: Voxel-based thickness analysis of intricate objects, *International Journal of CAD/CAM*, 6(1), 2006, 105–115.
 - [18] Thompson, D.; Crawford, R.: Computational quality measures for evaluation of part orientation in freeform fabrication, *Journal Of Manufacturing Systems*, 16(4), 1997, 273–289. [http://dx.doi.org/10.1016/S0278-6125\(97\)89098-X](http://dx.doi.org/10.1016/S0278-6125(97)89098-X)
 - [19] Wen, X.; Huang, J.; Wang, F.; Sheng, D.: Conicity and cylindricity Error Evaluation Using Particle Swarm Optimization, *Precision Engineering*, 34(2), 2010, 338–344. <http://dx.doi.org/10.1016/j.precisioneng.2009.08.002>
 - [20] Xu, F.; Wong, Y.; Loh, H.; Fuh, J.; Miyawaza, T.: Optimal orientation with variable slicing in stereolithography, *Rapid Prototyping Journal*, 3(3), 1997, 76–88. <http://dx.doi.org/10.1108/13552549710185644>
 - [21] Yang, Y.; Fuh, J.; Loh, H.; Wong, Y.: Multi-orientational deposition to minimize support in the layered manufacturing process, *Journal of Manufacturing Systems*, 22(2), 2003, 116–129. [http://dx.doi.org/10.1016/S0278-6125\(03\)90009-4](http://dx.doi.org/10.1016/S0278-6125(03)90009-4)
 - [22] Zhang, J.; Li, Y.: A unit sphere discretization and search approach to optimize building direction with minimized volumetric error for rapid prototyping, *International Journal of Advanced Manufacturing Technology*, 67(1–4), 2013, 733–743. <http://dx.doi.org/10.1007/s00170-012-4518-0>